Application of hot-wire anemometry for experimental investigation of flow distribution in micro-packed bed reactors for synthesis gas conversion

Farbod Dadgar[1], Hilde J. Venvik[1] and Peter Pfeifer[2]*

*peter.pfeifer@kit.edu (Correspondig author)

[1]Department of Chemical Engineering, Norwegian University of Science and Technology (NTNU), NO-7491 Trondheim, Norway

[2]Karlsruhe Institute of Technology (KIT), Institute for Micro Process Engineering (IMVT), Hermann-von-Helmholtz-Platz, DE-76344 Eggesnstein-Leopoldshafen, Germany

Highlights

Hot-wire anemometry (HWA) flow distribution measurement applied to micro-packed bed reactors

Measurements of flow distribution as a function of particle size distribution and particle size enabled

Potential bottlenecks of catalyst particles packing in microreactor identified

Application of hot-wire anemometry for experimental investigation of flow distribution in micro-packed bed reactors for synthesis gas conversion

Farbod Dadgar[1], Hilde J. Venvik[1] and Peter Pfeifer[2]*

*peter.pfeifer@kit.edu (Correspondig author)

[1]Department of Chemical Engineering, Norwegian University of Science and Technology (NTNU), NO-7491 Trondheim, Norway

[2]Karlsruhe Institute of Technology (KIT), Institute for Micro Process Engineering (IMVT), Hermann-von-Helmholtz-Platz, DE-76344 Eggesnstein-Leopoldshafen, Germany

The knowledge of the flow distribution inside microstructured reactors is valuable e.g. for improving the reactor design, developing flow distributors, and optimizing the catalyst loading method. The applicability of the hot-wire anemometry (HWA) technique for experimental determination of the flow distribution inside a multi-stack micro-packed bed reactor is demonstrated for the first time. The anemometry data is then evaluated in relation to the reactor performance for methanol synthesis under relevant industrial operating conditions. A 400 µm long hot-wire connected to a constant temperature anemometer was applied for scanning the flow out of a specially designed reactor model, clamped on a motorized table equipped with a precise positioning system. The anemometry measurements revealed a nonuniformity in the catalyst packing, partially resulting from the reactor design. The flow distribution is poorer for smaller particles and for wider particle size distributions, and worsens as the superficial flow velocity (and the pressure drop) decreases. The effects of the packing nonuniformity on the reactor performance appear minor under methanol synthesis conditions. They could, however, turn out significant upon pushing the overall conversion in the whole reactor towards equilibrium as the synthesis reaction is exothermic, and temperature increase does alleviate the problem. The reactor design should be modified instead.

Keywords

microstructured reactor, microchannel reactor, hot-wire anemometry, flow distribution, residence time distribution, gas-to-liquid, methanol synthesis

1 Introduction

Micro process technology has opened up new opportunities for process intensification through equipment size reduction, process simplification and process integration. Miniaturized flow dimensions and high surface-to-volume ratio in micro-units are the origin of promising characteristics such as enhanced heat and mass transfer and improved safety [Pohar and Plazl(2009), Mills et al. (2007) Borovinskaya and Reshetilovskii (2008), Matlosz and Commenge (2002)]. Portability, modularity, flexibility and high performance of microstructured reactors may facilitate the development of compact natural gas-, coal-, and biomass-to-liquid (XTL) technologies which are safe and economic in small scales and suitable for remote and offshore applications. This effort has been pioneered by e.g. Karlsruhe Institute for Micro Process Engineering (IMVT), Mainz Institute of Microtechnology (IMM), Pacific Northwest National Laboratory (PNNL), etc. and taken further to commercialization by companies like CompactGTL and Velocys. While there is a trend towards building larger GTL plants to benefit from economies of scale, such technologies may be the breakthrough required for competitive production of the easily-transportable fuels (e.g. methanol, dimethyl ether or Fischer-Tropsch liquids) from stranded/associated natural gas or gas produced from highly distributed bio-based feedstock that is not otherwise economically feasible to exploit.

Microstructured reactors can normally be considered as parallel arrays of identical channels. In general, uniform distribution of the flow among the microchannels is highly desirable in order to maximize the overall performance of the reactor [Commenge et al. (2002)]. Similarity of the size and geometry of channels (which directly affect the pressure drop) and

proper design of the reactor inlet are the most important factors for obtaining a uniform flow distribution. To emphasize the significance of identical channel size of flow distribution between different channels and reactor performance, [Pfeifer and Schubert (2007)] made a simple comparison between two parallel rectangular channels with 80 and 90 μm width, and their estimations showed 27% higher flow rate, 11% lower heat transfer area and 25% lower overall heat flux for the wider channel, both channels beeng connected to the same manifold. Such variations in channel size may be an outcome of fabrication tolerances or e.g. uneven catalyst coating. In the latter case, lower catalyst mass (thinner coating) in the channel with higher flow rate can lead to a higher load on the catalyst (2.5 times higher flow rate per catalyst mass for the previous example, assuming 10 and 5 μm thick coating) [Pfeifer and Schubert (2007)]. In the case of microstructured reactors packed with catalyst particles, a similar approach can be used to evaluate the significance of non-uniform catalyst packing for flow distribution among channels connected to the same manifold. Considering two identical parallel microchannels or also microsized slits with different bed porosities of 0.5 and 0.4, the flow rate through the channel with the higher void fraction is approximately 2.8 times higher than the one with the lower porosity, as estimated from the Ergun equation (Eq. 1) [Ergun (1952)] under laminar flow regime and conditions of identical pressure drop, where the second term is supposed to be negligible. Identical pressure drop for both channels is valid, as both are connected to a common inlet and outlet.

$$\frac{\Delta P}{L} = 150 \ \frac{\mu u_s (1-\varepsilon)^2}{d_p^2 \varepsilon^3} + 1.75 \ \frac{\rho u_s^2 (1-\varepsilon)}{d_p \varepsilon^3} \tag{1}$$

where ΔP is the pressure drop, L is the length of the channels, μ and ρ are respectively the viscosity and density of the fluid, ε is the void fraction (porosity) of the catalyst bed, u_s is the superficial velocity, and d_p is the average diameter of the catalyst particles. At the same time, according to Eq. 2, there is ~16% less catalyst mass in the channel with the higher void fraction and higher flow rate:

$$\varepsilon = 1 - \frac{\rho_b}{\rho_p} \tag{2}$$

where ρ_b and ρ_p are respectively bed (bulk) density and catalyst particle density. Overall, these simple calculations suggest that an increase in the bed porosity from 0.4 to 0.5, can lead to almost 240% increase in the flow rate per catalyst mass between the two channels with common manifold. The total performance loss depends also on other factors such as reaction kinetics, endo/exothermicity, and thermodynamic limitations, and may be significant.

Knowledge about the flow distribution in microstructured reactor is useful for prediction of the reactor behavior and optimization the reactor design, inlet geometry and catalyst loading method. Laser Doppler anemometry (LDA) is an experimental technique that has been applied for determination of flow distribution in microstructured reactors, supplementary to CFD simulations [Rebrov et al. (2007), Mies et al. (2007)]. However, for the small measurement volumes and the low velocities corresponding to micro-units, application of LDA to gas streams is complicated and not very accurate. Therefore, to apply the method for studying the flow in micro-units, the gas stream may be replaced by liquid flow with identical Reynolds numbers, as suggested by Schouten et al. [Rebrov et al. (2007), Mies et al.(2007)]. Apart from the complications associated with the use of liquid and possible errors that may be introduced by fluid substitution, such approaches may not be appropriate for micro-packed bed reactors where liquid flow may affect the catalyst packing or even deagglomerate the catalyst particles and wash them out of the reactor.

[Pfeifer et al. (2004)] developed an experimental technique based on hot-wire anemometry that is accurate for investigation of gas flow distribution in microstructured units. The technique makes use of a precise positioning system and a small hot-wire (probe) connected to a constant-temperature anemometer. The probe is being moved in front of and parallel to the reactor outlet to scan the flow passing through the individual channels. The applicability of the method has been demonstrated for quantitative analysis of the flow distribution in one- and two-dimensional arrays of wall-coated microchannels [Pfeifer et al. (2004), Pfeifer and Schubert (2007)]. In addition, the method can be used for non-destructive evaluation of the catalyst coating uniformity.

Hot wire (thermal) anemometry is a well established experimental technique (see e.g. [Bruun (1995)]) where a thin wire, heated by electric current, is exposed to a stream of fluid

(with constant temperature and composition) and the power needed for heating the wire correlates with the heat loss from the wire, which in turn is a function of the flow velocity. The principle governing equation can be written as follows:

$$P = Q_{cv} + Q_{co} + Q_r \tag{3}$$

where P is the power for Joule heating and is equal to V^2/R (with V being the voltage drop across the wire and R the wire electrical resistance), and Q_{cv}, Q_{co} and Q_r are convective, conductive and radiative heat losses from the hot-wire, respectively. [King (1914)] suggested a simple relation between the flow velocity and the conductive heat transfer coefficient (h) from an infinite cylindrical body in a flow at low Reynolds number, known as King's law (Eq. 4),

$$Q_{cv} \propto h \propto a + b\ u^{0.5} \tag{4}$$

where a and b are constants and u is the flow velocity. In constant-temperature anemometers, the hot-wire is connected to a Wheatstone bridge, and a servo amplifier keeps the bridge in balance by controlling the current to the probe (keeping the electrical resistance (R) of the hot-wire and hence its temperature constant). At constant fluid temperature, and when heat loss by radiation and conduction from two ends of the wire are either negligible or independent of the flow velocity, Eq. 3 can be rewritten as;

$$V^2 = A + B\ u^{0.5} \tag{5}$$

where V is voltage drop across the probe, u is fluid velocity and, A and B are constants that can be obtained through calibration of the probe in known flow velocities.

Micro-packed bed reactors have been studied in our collaboration for conversion of synthesis gas to methanol [Bakhtiary-Davijany et al. (2012) Bakhtiary-Davijany et al. (2011-1), Bakhtiary-Davijany et al. (2011-2)], dimethyl ether [Hayer et al. (2013) Hayer et al. (2011-1), Hayer et al. (2011-2)], and Fischer-Tropsch products [Myrstad et al. (2009)], and established as

practically isothermal, isobaric and free from mass transfer limitations. The residence time distribution (RTD) in the reactors has also been investigated theoretically, and with the assumption of uniform catalyst packing throughout the reactor and uniform flow distribution among the micro-slits (see section 2.1), a narrow RTD was estimated [Bakhtiary-Davijany et al. (2011-1), Bakhtiary-Davijany et al. (2011-2), Hayer et al. (2013)]. The assumptions were based on visual observation of the catalyst packing in a glass model reactor and also the high reproducibility of the reactor performance when re-packed with a new batch of the same catalyst. Nevertheless, as stressed by the authors [Bakhtiary-Davijany et al. (2011-1) Bakhtiary-Davijany et al. (2011-2)], validation of these assumptions requires an experimental investigation of the flow distribution.

In the present study, the flow distribution in a micro-packed bed unit, similar to the microstructured reactors (MSR) applied in our earlier study, is investigated experimentally using hot-wire anemometry. The results are then discussed in relation to the MSR performance for methanol synthesis from synthesis gas.

2 Experimental

2.1 Microstructured units

An integrated micro-packed bed reactor-heat exchanger (Fig. 1), referred to as the microstructured reactor (MSR), was used for methanol synthesis. The MSR is made of stainless steel and fabricated in the Institute for Micro Process Engineering (IMVT), Karlsruhe Institute of Technology (KIT), Germany. The reactor consists of 8 parallel reaction slits, 60 mm long and with rectangular cross-section of 0.8 mm×8 mm. A series of cylindrical pillars with diameter of 0.8 mm and center-to-center distance of 1.6 mm are positioned inside each slit in a hexagonal arrangement. Each slit is sandwiched between two series of cross-flow channels for circulation of heat transfer oil. The oil channels have rectangular cross-section of 0.25 mm×0.50 mm and are separated by 0.25 mm-thick fins. Fig. 2 demonstrates the principle design of the reactor. Two porous metallic plates (frits) were used at the inlet and outlet of the reaction section to hold the catalyst bed in place and to improve flow distribution into the slits.

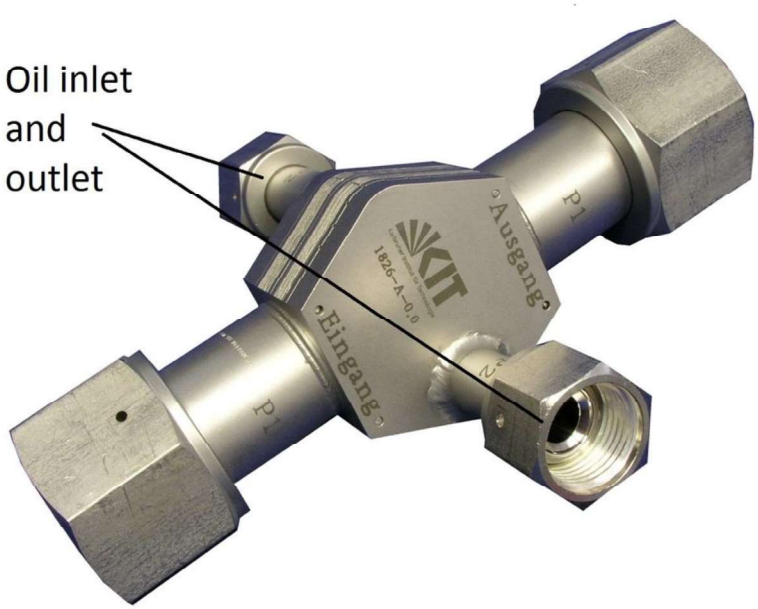

Figure 1: Photo of the microstructured reactor (MSR) used for methanol synthesis.

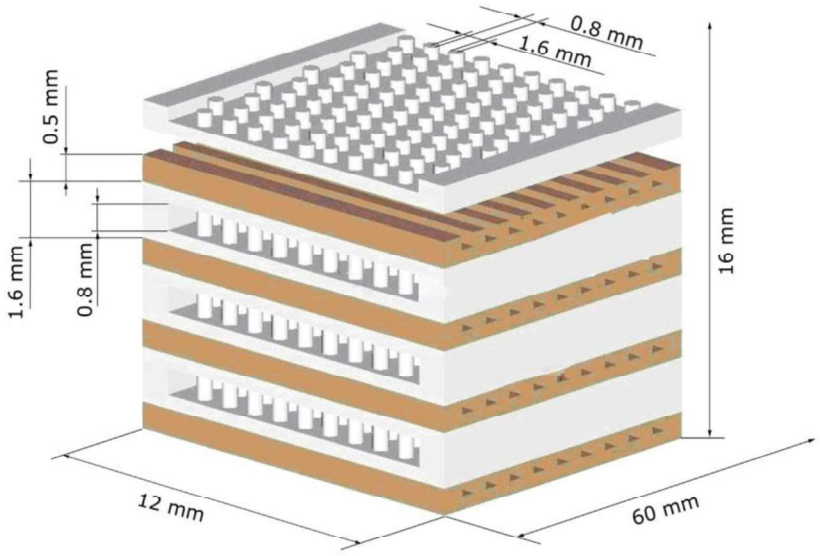

Figure 2: Principle design of the microstructured units with reaction slits (white color) and oil channels (brown color).

A replica of the MSR with similar design and dimensions, but different configuration at the outlet, was used for investigation of the flow distribution in the reactor. It is termed the

microstructured body (MSB), and a photo is presented in Fig. 3. The 8 slits of the MSB are blocked (not etched) at one end with a 1 mm thick wall and a row of 13 channels (per slit) is cut into the wall at half height of the slit, creating a network of 8×13 channels for the gas flow out of the MSB. These channels have rectangular cross-section of 0.4 mm×0.03 mm and are distanced ~0.13 mm apart from the adjacent channels in the row and ~2 mm apart from the adjacent rows. The design of the reaction slit and the configuration of the outlet channels are demonstrated in Fig. 4. Similar to the MSR, a frit is fastened to the MSB inlet.

Figure 3: Photo of the microstructured body (MSB) used in hot-wire anemometry measurements.

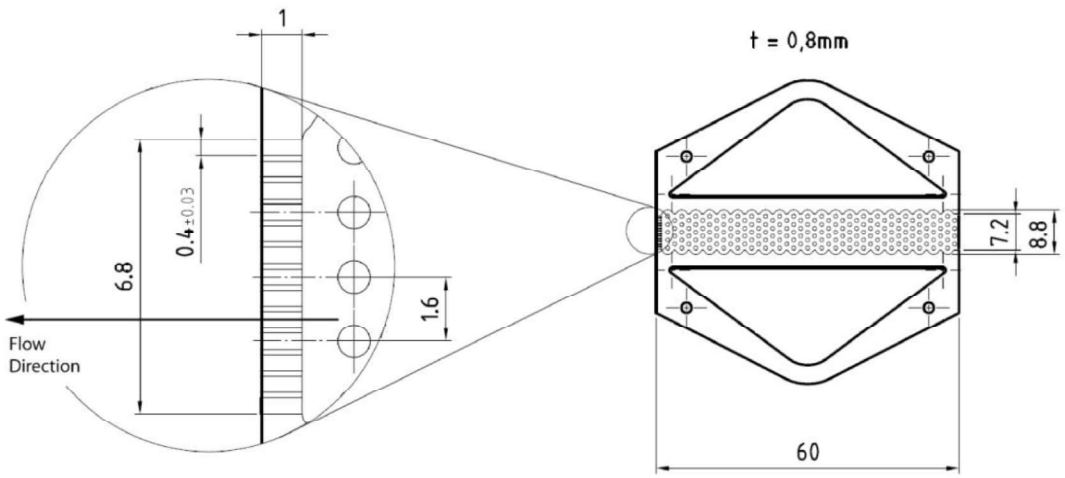

Figure 4: The design of the slits in the microstructured body (MSB). The slits' size and geometry are identical to the ones of the MSR, except for the outlet configuration (magnified in the left panel). All dimensions indicated are in millimeters.

A homemade and a commercial methanol synthesis catalysts were used for methanol synthesis experiments and hot-wire anemometry measurements, respectively. Catalyst pellets were crushed and sieved to a desirable particle size range and loaded into the MSR or MSB by putting small amounts of the catalyst powder on top of the reaction slits and gently knocking and shaking the reactor until it is completely filled. The use of ultrasound application for catalyst loading was also evaluated, by clamping an ultrasonic transducer around the MSB's main section (on top of the slits) while loading the catalyst. The quality of the catalyst packing inside the slits was also examined visually using a glass model of the reaction slit, as shown in Fig. 5.

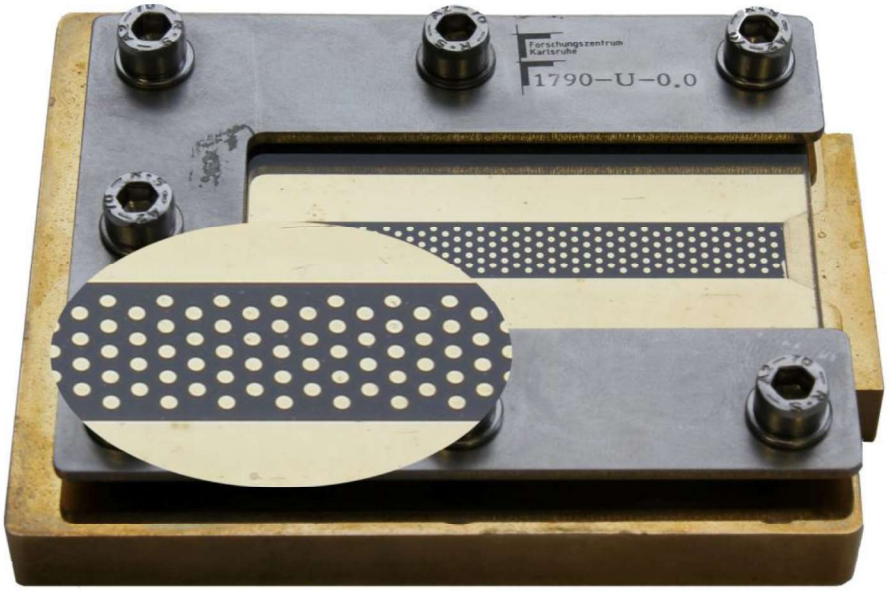

Figure 5: Packing of the commercial methanol synthesis catalyst (50-200 μm) inside the slit model.

2.2 Methanol synthesis setup

The homemade $Cu/ZnO/Al_2O_3$ methanol synthesis catalyst was prepared through a conventional coprecipitation method, as described elsewhere [Dadgar et al. (2015)]. Methanol was synthesized in the MSR from a premixed synthesis gas with $H_2/CO/CO_2/N_2$ molar ratio of 65/25/5/5 mol% (module ”M" of 2), supplied by Yara Praxair. Feed flow rate and reactor pressure were controlled using, respectively, a digital mass flow controller and a digital back pressure controller (from Bronkhorst). The reactor was heated through circulation of heat transfer medium in the oil channels using a Julabo circulator equipped with a built-in temperature controller. The reaction temperature was monitored by inserting three thermocouples into dedicated holes on the reactor body (on top of, and along the slit centerline) which provide close proximity (∼2 mm) to the catalyst bed. Liquid products, consisting of mainly methanol and water, were condensed in a cold pot and gas products were analyzed online in an Agilent 5890 gas chromatograph. Carbon mass balance over the setup always closed with an error of less than 5%. Prior to syngas introduction, the catalyst was reduced in situ with diluted H2 (3%) over a 12 h-long step-wise temperature increase, followed

by 5 h dwell at 255°C. Methanol synthesis was conducted at 215-275°C, 80 bar, and space velocity of 150-1200 Ncm ^{3}/min/g $_{catal.}$.

2.3 Hot-wire anemometry setup

The MSB was clamped horizontally to a three-axis motorized stage from Physik Instrumente (PI), which enables controlled movements of the MSB in x/y/z directions with nanometric increments. Movements of the stage are controlled through a computer and the precision with regard to reset the positioning system to the identical point in space is around 2 μm. A 400 μm-long hot-wire with diameter of 2.5 μm from Dantec Dynamics is used. The probe is connected to a constant-temperature anemometer which keeps the wire temperature constant at 280°C throughout the measurements. The probe is attached to a rotating element which allows for axial rotation of the probe, changing the wire alignment from horizontal (useful for positioning) to vertical (for measurements). A stereomicroscope (M3C Wild Heerbrugg) is used for initial positioning of the probe.

Anemometry measurements were done at ambient conditions using flow of air in the range of 600-2400 Ncm^3/min, leading to a Reynolds number range of 27-108 in the slits (assuming rectangular channels with identical height and cross sectional area as the slits) and 29-116 in the outlet channels. The air flow rate to the MSB was controlled using a (Brooks) digital mass flow controller, and the pressure drop over the microstructured body was measured using a pressure gage connected to the MSB inlet. The hot-wire was positioned vertically, i.e. perpendicular to the outlet channel row, with its center aligned vertically with the row, and distanced $\sim$150 μm away from the MSB outlet. That means that all experiments have been conducted at ambient pressure outlet conditions. Fig. 6 shows photos of the probe in front of the MSB outlet. The micro structured body was moved horizontally with 5 μm/s speed allowing the probe to scan all outlet channels in a row before being moved to the next row. The probe and the MSB were covered from the sides to reduce noise in the measurements.

a)

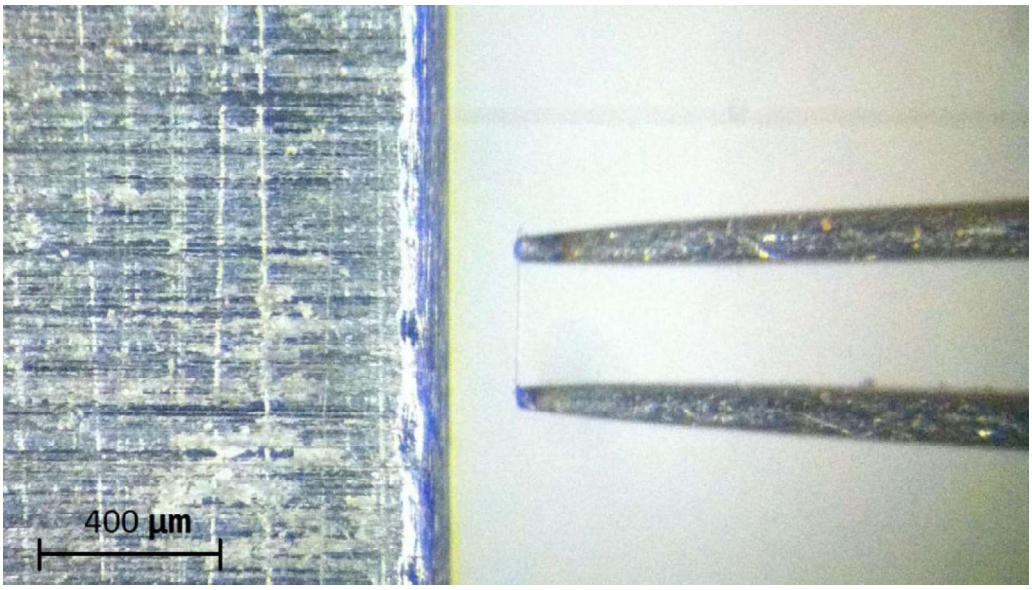

b)

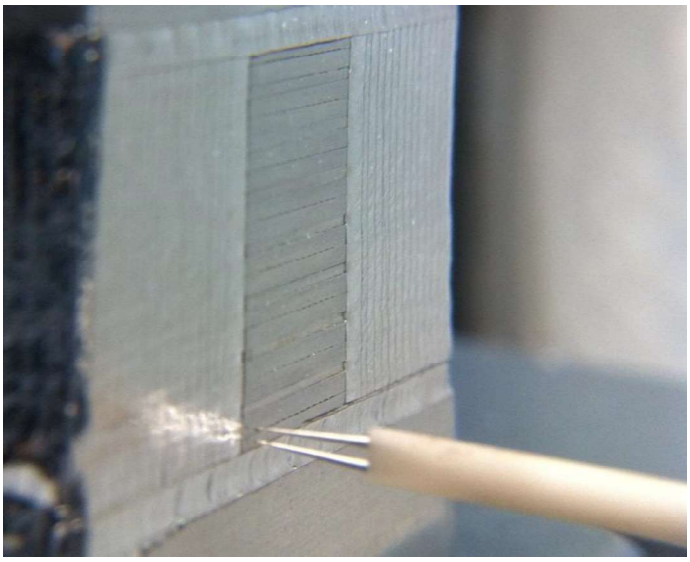

Figure 6: The 400 μm long hot-wire in front of the MSB outlet; a) the view from above through the microscope during initial positioning, and b) the view from the side during measurements.

The voltage was measured with a frequency of 500 Hz, and each data point was an average of 512 measurements. That, with the 5 μm/s screening speed, results in ~80 data points per outlet channel. Fig. 7 shows two typical hot-wire anemometry measurement data recorded along one row of channels, sorresponding to a single reactor slit filled with catalyst.

The gas flow rate through each channel was calculated using the mean value of the measured voltage across that channel, using Eq. 5.

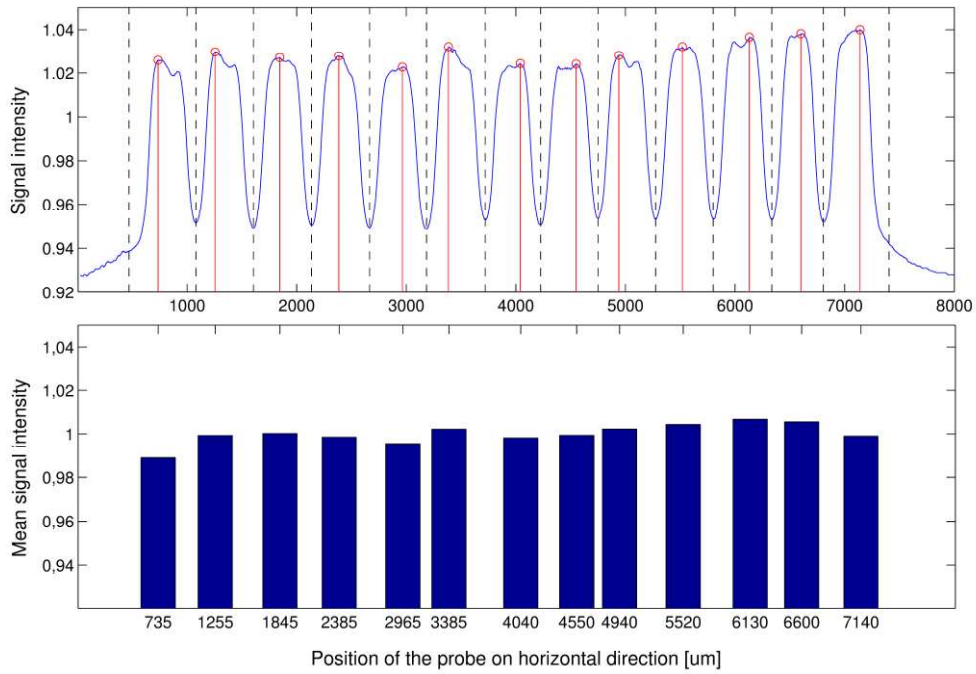

a)

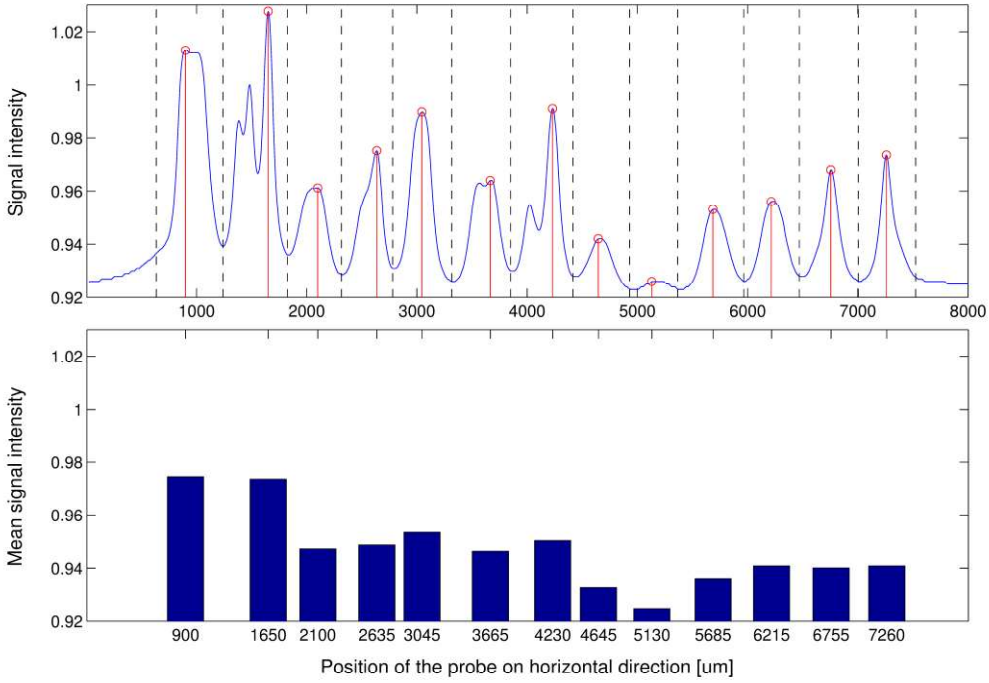

b)

Figure 7: Anemometer signal intensity (voltage) recorded for two different rows of channels (a and b), each exemplifying one reactor slit. The upper panels show the signal measured along the row where each peak represent one of the 13 outlet channels. The lower panels show the

voltage signal corresponding to each channel averaged between the two local minima indentified from the upper panel (dotted lines) and positioned horizontally at the maximum intensity position (red lines). The channel width (integral interval) for the first and last channel in a row is assumed equal to the averaged length of the other 11 channels.

Considering the wire length of 400 μm and the relatively small channel width of 30 μm, it is apparent that only a portion of the hot-wire is exposed to the flow at a distance of $\sim$150 μm to the channel outlet. Fig. 8 shows changes in the recorded signal intensity in front of the midsection of a randomly chosen middle channel (7th channel in row 4) while moving the MSB away from the probe. Intensity of the signal first increases, as larger part of the wire became exposed to the flow, and then decreases as the flow velocity drops away from the channel outlet. To limit the overlap from the adjacent channels ($\sim$130 μm distance in x direction), the probe-MSB distance was chosen as 150 μm. However, in practice the distance varied in the range of 120-200 μm, due to MSB misalignment relative to the probe. The error of the calculated flow rates caused by such deviations is expected to be small (always less than 3% in several randomly tested channels under total flow rate of 1.2 L/min) and can hence be neglected.

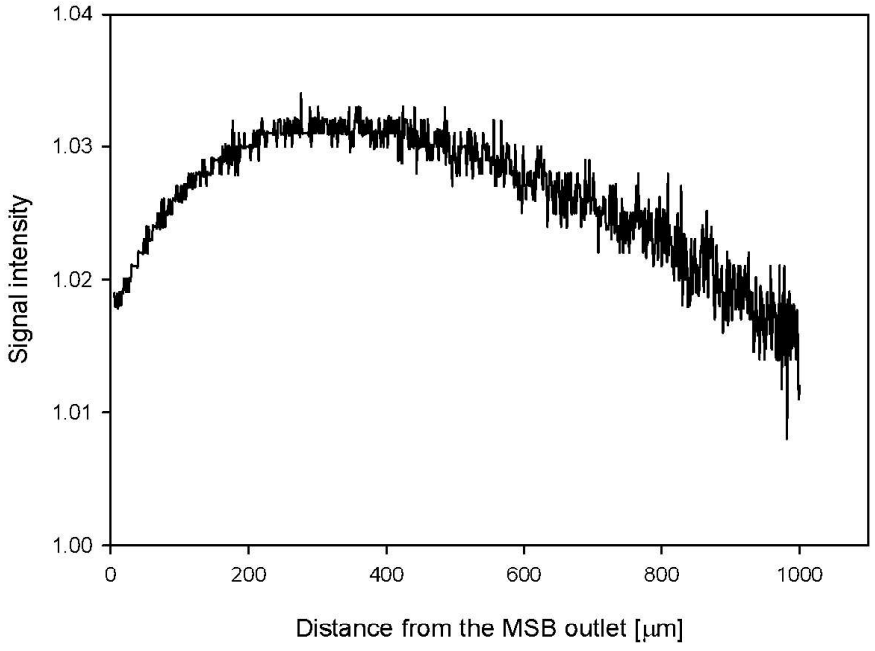

Figure 8: Dependence of the anemometer signal intensity on the hot-wire distance to the microstructured body (MSB) outlet.

Calibration of the signal intensity versus the flow rate and the corresponding velocity from the outlet of the tiny channels is therefore not applicable and a classical voltage versus an homogeneous velocity field does not make sense. To provide a relation between flow rate and signal the suggestion from [Pfeifer et al. (2004)] has been reproduced. The mean of signal maxima has been correlated towards the overall flow rate through the MSB using equation 5. This is of course only possible for experiments where the deviation between the channels is low. Further details on the accuracy of this approach is discussed in section 3.3.

3 Results and discussion

3.1 Flow distribution

Fig. 9 shows the flow distribution in the empty microstructured body (MSB). The measurements were performed twice and at three different air flow rates of 0.6, 1.2 and 2.4 NL/min, and results are presented as the percentage of the total flow rate, i.e. written as normalized flow, through each of the 13 outlet channels of the 8 slits (rows). The results show an uneven distribution of the flow among the empty slits, but rather uniform flow across each slit. The flow distribution becomes more uniform with an increase in the total flow rate, which also results in an increase in the pressure drop over the MSB from 14 mbar under the lowest flow rate, to 48 mbar for the highest. Considering the small size of the outlet channels (0.4 mm×0.03 mm) and the expected fabrication tolerances (~0.01 mm), dimensional variations among the tiny outlet channels is most likely the cause of the flow maldistribution. Effects of dimensional variations in absence of a catalyst particle packing in the corresponding MSR, which does not contain the tiny outlet channels, are likely negligible due to much lower fabrication tolerances in relation to the absolute size of the slits.

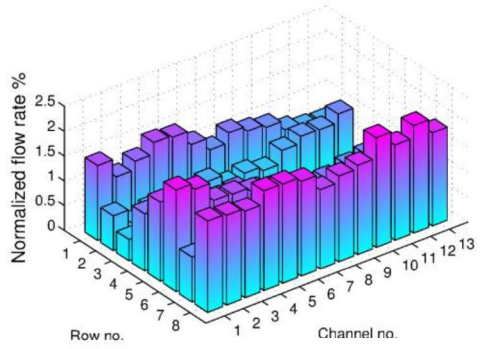

a) 0.6 L/min, ΔP=13.8 mbar (run 1)

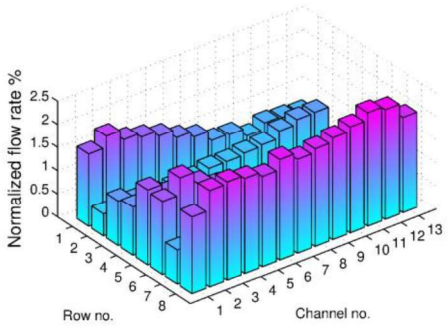

b) 0.6 L/min, ΔP=14.1 mbar (run 2)

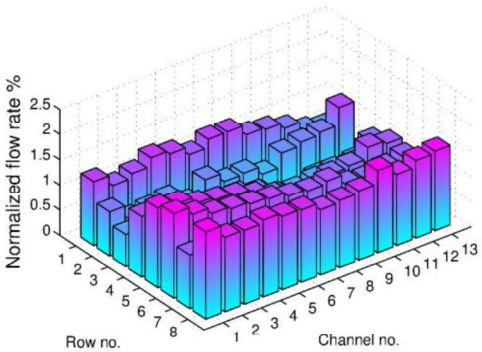

c) 1.2 L/min, ΔP=23.9 mbar (run 1)

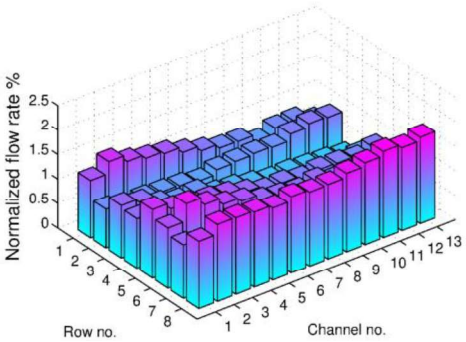

d) 1.2 L/min, ΔP=24.0 mbar (run 2)

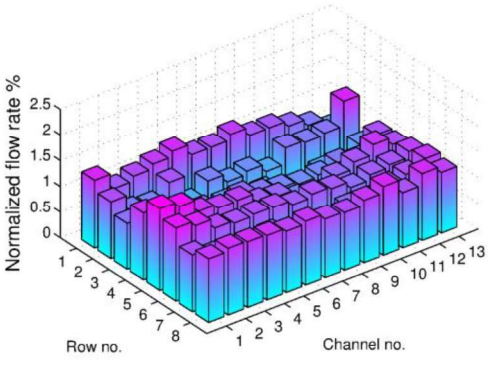

e) 2.4 L/min, ΔP=48.2 mbar (run 1)

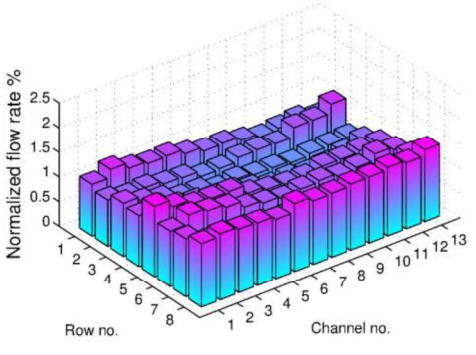

f) 2.4 L/min, ΔP=47.9 mbar (run 2)

Figure 9: Flow distribution in the empty microstructured body (MSB) under the total air flow rate of (a, b) 0.6, (c, d) 1.2 and (e, f) 2.4 L/min from two separate measurements (run 1 and 2). Flow through each channel (13 outlet channels for each of the 8 slits) is indicated as the percentage of the total flow.

The flow distribution measurements in the MSB packed with methanol synthesis catalyst are presented in Fig. 10. Two different particle size ranges, 50-80 μm and 100-200 μm, were applied under total air flow rate of 0.6, 1.2 and 2.4 NL/min. In comparison to the results with the empty MSB, the air flow seems to distribute more evenly among the 8 slits, although the flow distribution inside each slit widens after packing the MSB with catalyst. These results suggest, firstly, that the effect of dimensional variations of the outlet channels on the flow distribution is negligible in the packed MSB, since the pressure drop caused by the catalyst bed is much higher than the pressure drop over the empty MSB (see later). Secondly, the flow rate along the sidewalls of the packed slits is higher, likely due to a lower packing density (higher bulk porosity) close to the sidewalls of the slits. Considering the design of the slits (see Fig. 4), this may be explained by a lower probability for the catalyst particles to enter the space between the slits' sidewall and the first/last pillars in a row. As with the empty MSB, the flow distribution improves by increasing the total air flow rate, which also leads to an almost linear increase of the pressure drop. Applying a larger catalyst particle size results in a narrower flow distribution in the MSB, while causing a lower pressure drop. This may suggest a more uniform packing inside the slits when larger particle size is used, likely due to a smaller surface energy of the particles (lower surface-to-volume ratio) leading to less agglomeration and easier loading of the particles.

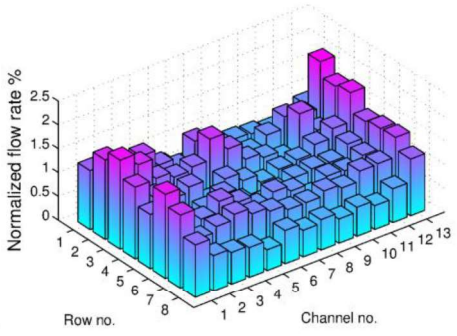

a) 0.6 L/min, 50-80 µm, ΔP=2.0 bar

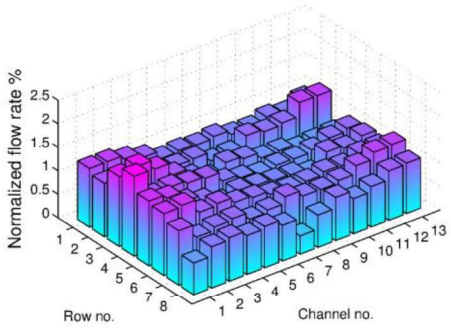

b) 0.6 L/min, 100-200 µm, ΔP=235 mbar

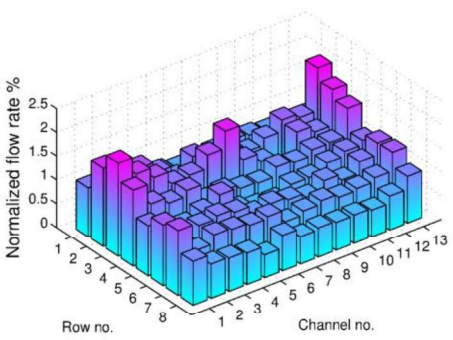

c)

1.2 L/min, 50-80 µm, ΔP=2.9 bar

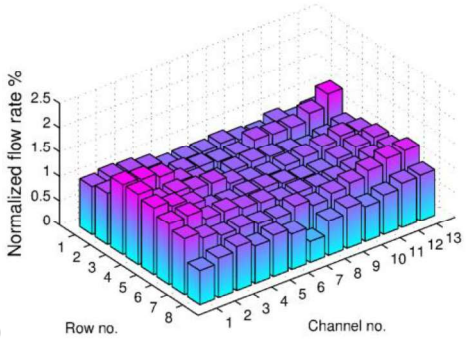

d)

1.2 L/min, 100-200 µm, ΔP=410 mbar

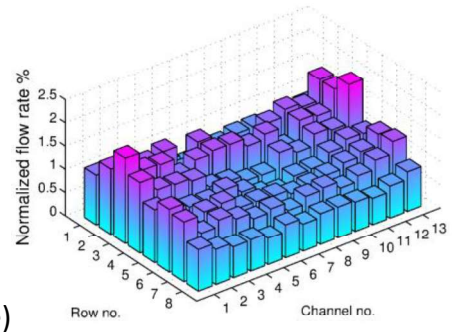

e)

2.4 L/min, 50-80 µm, ΔP=4.4 bar

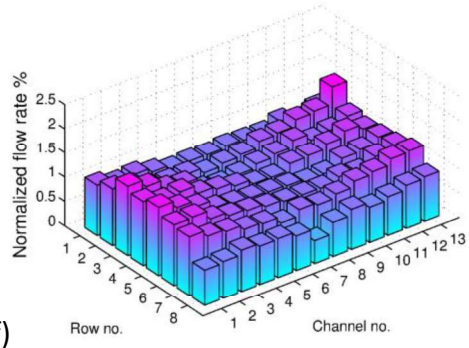

f)

2.4 L/min, 100-200 µm, ΔP=759 mbar

Figure 10: Flow distribution in the packed microstructured body (MSB). Measurements were done with two different catalyst particle sizes of 50-80 or 100-200 μm, under total air flow rate of 0.6, 1.2 and 2.4 NL/min. Flow through each outlet channel is presented as a percentage of the total flow rate.

Fig. 11 demonstrates the flow distribution in the MSB packed with a 50:50 wt% mixture of the 50-80 μm and the 100-200 μm sized catalyst particles. The reproducibility of the catalyst packing was examined by repeating the anemometry measurements 4 times, each time after repacking the MSB with a new batch of the same catalyst mixture. For the last experiment, ultrasound agitation was used during the catalyst loading. While there is some variation/deviation between reproductions, they all point to the same general conclusion that the flow channeling along the slit walls is a much bigger issue when a wider catalyst particle size distribution is used. Use of ultrasound for loading the catalyst into the MSB does not have a

significant effect on uniformity of the catalyst packing and the flow distribution. On the contrary, while the ultrasound application densifies the packing, it does not seem to assist the particles transport towards the sidewalls, therefore it creates an even bigger gap between the packing density near the sidewalls and in the slit midsection.

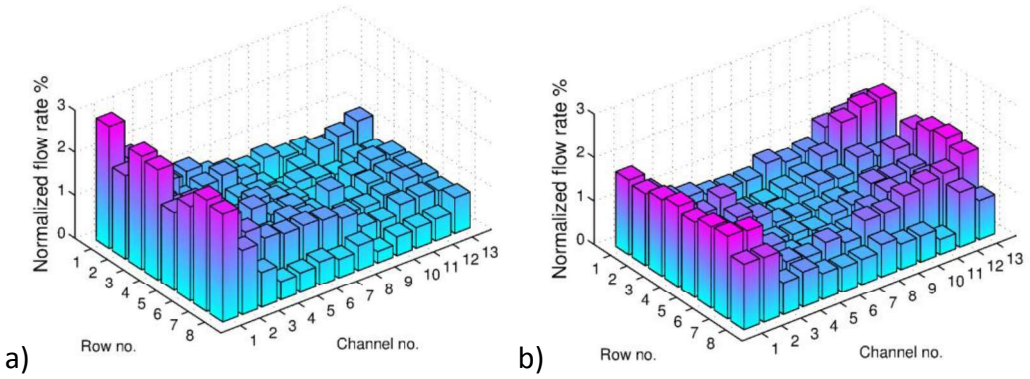

a) Run 1, ΔP=817 mbar

b) Run 2, ΔP=949 mbar

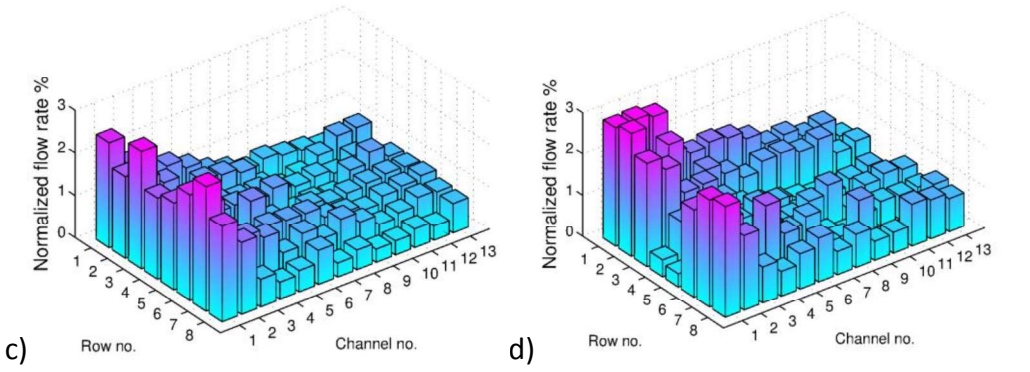

c) Run 3, ΔP=850 mbar

d) Run 4, ΔP=1372 mbar, w/ultrasound agitation of catalyst

Figure 11: Flow distribution in the MSB packed with a 50:50 wt% mixture of 50-80 µm and 100-200 µm sieved catalyst particle fractions under 0.6 NL/min total air flow. The flow rate through each outlet channel is normalized against the total flow rate. Measurements are repeated 4 times, repacking the MSB each time. Run 4 is performed with the MSB packed applying ultrasound agitation.

The pressure drop along the MSB as a function of the space velocity (total flow rate divided by the MSB volume, i.e. $\sim$2 cm ^{3}) is presented in Fig. 12 for all the performed experimental conditions applied. The volume has been defined as open void for catalyst and has been calculated from the design specifications and not from filling the MSB with liquid. For the precision of the absolute values this might result in a absolute deviation of less than 10 % in volume. As expected for a laminar flow regime, the pressure drop increases linearly with total air flow rate. Moreover, and also as anticipated, smaller size of the packed particles leads to a higher pressure drop,. Use of ultrasound agitation during catalyst loading led to an increase in the pressure drop of the bed which could be due to a reduction in the average particle size (de-agglomeration of the particles), a reduction in the void fraction of the bed (increased packing density), or both. As implied from Figs. 10 and 11, however , these larger pressure drops are, not associated with a more uniform flow distribution.

For the sake of comparison, the pressure drop was also estimated from the Ergun equation (Eq. 1) and the result is presented in Fig. 12 for average particle size of 65 μm. The porosity of the bed was estimated using Eq. 6, proposed by [Haughey and Beveridg (1969)] for a bed of spherical particles.

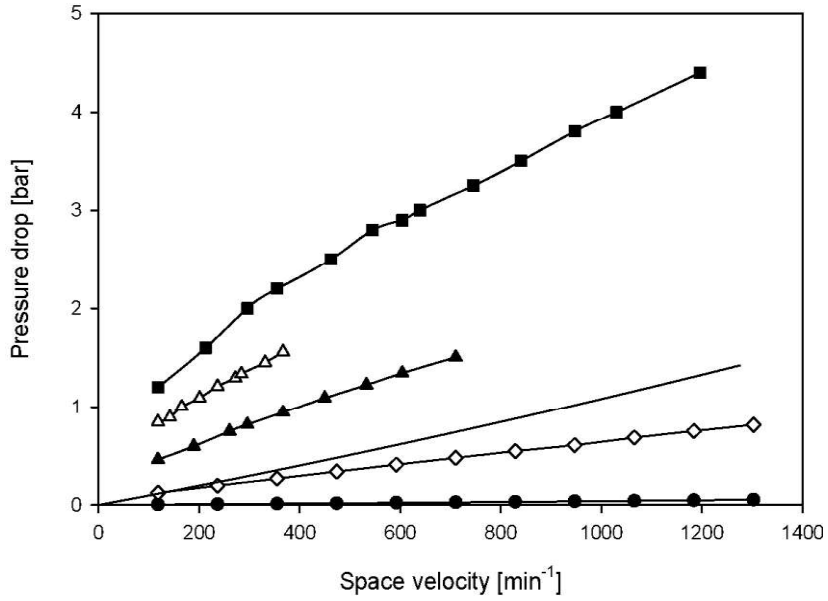

Figure 12: Pressure drop of the air stream as a function of the space velocity over the empty

MSB (•), and MSB packed with catalyst with particle size of 50-80 μm (▪) , 100-200 μm (◊) (⋄), and 50-200 μm without (▲) or with (Δ)applying ultrasound during catalyst loading. The solid line shows theoretically estimated pressure drop over the MSB packed with 50-80 μm sized particles and bed porosity of 0.51, using Ergun equation; ambient temperature 22 °C.

$$\varepsilon = 0.38 + 0.073\left(1 + \left(\frac{D_h/d_p - 2}{D_h/d_p}\right)^2\right) \quad (6)$$

where d_p is the average particle size and D_h is the hydraulic diameter of the MSB slit (assuming a rectangular channel with identical height and cross sectional area as the slit). The porosity may also be obtained experimentally according to Eq. 2, where the particle density, ρ_p, is measured according to Archimedes' principle, and the bulk density, ρ_b, is known from the total MSB volume (~2 cm ^{3}) and the mass of the catalyst loaded (~1.6 g). The mean bulk porosity obtained for the MSB catalyst bed with particle size of 50-80 μm is 0.51 and 0.76 for the theoretical and experimental estimates, respectively. The calculated pressure drop is lower than the measured values for the correspondin particle size range (50-80 µm), as well as for the wider particle size distribution (50-200 µm) with and without ultrasound agitation-assisted packing, but less than the pressure drop measured for the larger particle size range (100-200 µm). This might be explained by the special configuration of the MSB outlet (narrow outlet channels with ~30 μm width) which can be partially blocked by catalyst particles, as well as by deviation of the particles shape from spherical shape and their size from the roughly defined average value.

3.2 Catalysis

Fig. 13 shows the effect of catalyst particle size on synthesis gas conversion to methanol at varying reaction temperature under constant gas flow rate and at constant temperature under varying gas flow rate. The synthesis was conducted under 80 bar pressure and total syngas flow rate in the range of 0.1-1.2 NL/min. All the three applied particle sizes, i.e. 50-80, 80-125, and 125-200 μm, yield comparable syngas conversion levels and further

interpretation of the data is rather speculative as variations are in approximately the same range as of the data accuracy. With that said, the results may suggest a slight decrease in the CO conversion by increasing the catalyst particle size, at otherwise identical conditions. The same trend has also been observed in the results of a similar set of experiments with direct syngas conversion to dimethyl ether at 50 bar and in a comparable microstructured reactor consists of one slightly larger reaction slit (8.8 mm×1.5 mm×60 mm) without pillars [Hayer et al. (2013)].

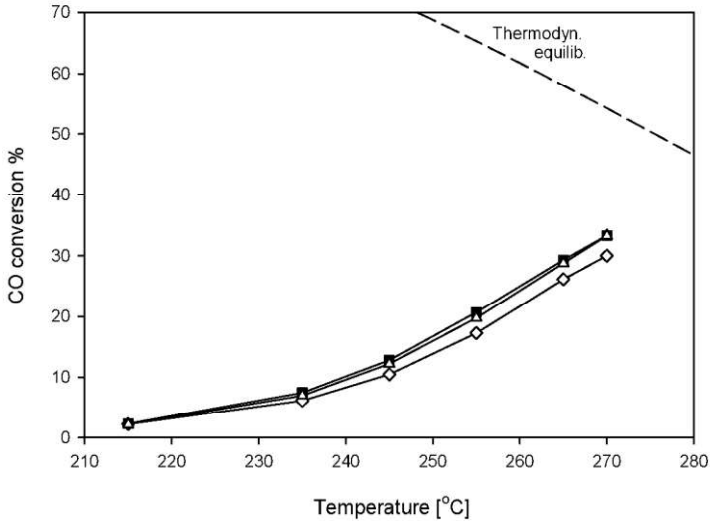

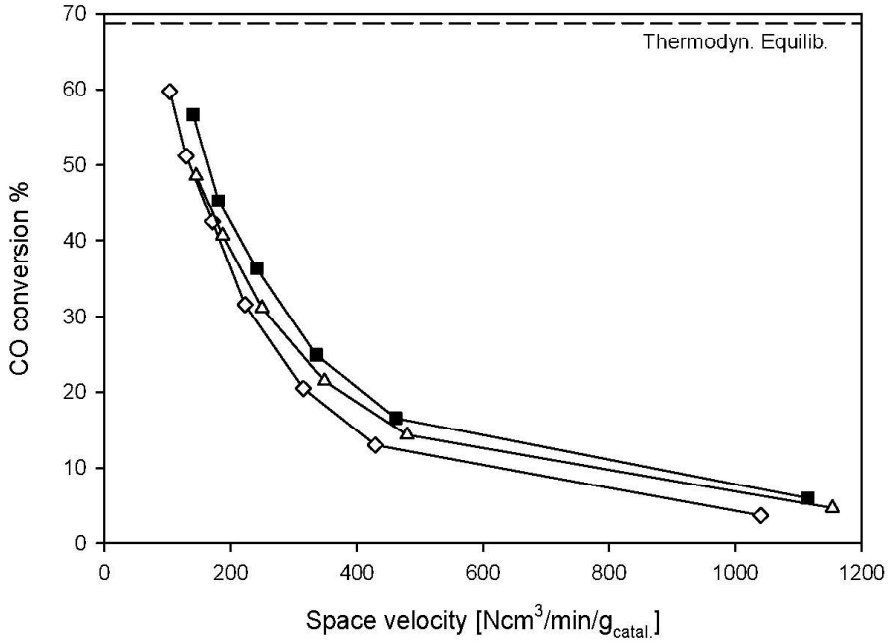

Figure 13: CO conversion at 80 bar total pressure for three different methanol synthesis catalyst particle size ranges; 50-80 μm (▪), 80-125 μm (Δ), and 125-200 μm (◊). (a) as a function of reaction temperature at 350 Ncm ^{3}/min/g $_{\text{catal.}}$ space velocity and (b) against space velocity at 255 °C.

At constant gas flow rate (Fig. 13a), increase in the reaction temperature and hence reaction rate widens the gap between the CO conversion for the largest catalyst size (125-200 μm) and for the two smaller particle sizes. This may be an indication that at high conversion levels, intra-particle mass transfer (pore diffusion) can affect the apparent methanol synthesis rate when catalyst particles are larger than 125 μm, under the conditions applied. The slight influence of the pore diffusion on the methanol synthesis rate has been reported for catalyst sizes in the range of 150-200 μm [Lommerts et al. (2000), Graaf et al. (1990)]. The observed effect of the catalyst size on the conversion is in the opposite direction as it would be expected based on the anemometry measurements, i.e. with a larger particle size the flow distribution is narrower and hence, the reactor performance may be superior. The lower CO conversion level despite a possibly better flow distribution in the reactor packed with larger particles may translate to an even stronger effect of the pore diffusion on the reaction rate than apparent from Fig. 13.

All in all, the methanol synthesis experiments do not seem to confirm any large variations in the overall reactor performance due to the applied changes in the catalyst particle size, and the corresponding variations in packing that the flow measurements seem to imply. This is consistent with previously obtained high reproducibility of methanol synthesis data [Bakhtiary-Davijany et al. (2011-1) Bakhtiary-Davijany et al. (2011-2)] in similar microreactor configurations, which would not be possible if the reactor performance under the applied conditions was highly sensitive to such changes. However, this neither confirms a uniform catalyst packing or an even flow distribution throughout the reactor, but that effects of the catalyst particle size and deviations in packing density are small at the applied reaction conditions. To clarify, it is useful to note that under the high pressure applied for the methanol synthesis (80 bar), the flow velocity and pressure drop is considerably lower than for similar gas flow rates applied at near-ambient conditions (as for the anemometry measurements). For

instance, at 1.2 NL/min, the Reynolds number in the slit is ~1 and the pressure drop is ~7 mbar under 80 bar, as opposed to 54 and 25 mbar, respectively, under ambient pressure. In other words, application of a larger particle size with a narrow size distribution (in the range examined) contributes to a uniform flow distribution in the reactor, as observable at rather high flow velocities and pressure drops, but the gain seems to be negligible at low velocities.

Moreover, judging from the the anemometry measurements at ambient pressure, the lower flow velocities and lower pressure drops suggest a poorer flow distribution inside the reaction slits under reaction conditions. However, this may not directly translate to a wide residence time distribution and poor reactor performance. The design of the slits and the presence of the pillars are known to promote the flow mixing inside the slit, balancing the effect of poor flow distribution [Bakhtiary-Davijany et al. (2011-1), Bakhtiary-Davijany et al. (2011-2), Hayer et al. (2013)]. Nevertheless, as the conditions at the reactor outlet approach the thermodynamic equilibrium, the influence of the flow maldistribution on the reactor performance may become significant in case of a exothermic reaction.

3.3 Accuracy of the anemometry data analysis

As discussed earlier, velocity or flow rate (assuming identical channel cross-sections) of the stream impinged on the hot-wire correlates with the voltage drop across the wire (signal intensity) according to Eq. 5. Values for the constants A and B in Eq. 5 should be obtained through calibration of the probe. However, since only a portion of the wire is exposed to the flow, direct calibration of the probe is not straightforward. Moreover, the assumptions of the King's law (Eq. 4), i.e. uniform temperature and flow velocity along the probe, may hold only over a portion of the hot-wire (almost constant length for all measurements). Conductive heat transfer from both ends of this "active" portion subject to the flow can be considerable and may vary with the flow velocity. Therefore, the actual flow rate may deviate largely from the one predicted.

With all that said, the applicability of the Eq. 5 for calculation of the flow rates from the measured signals has been investigated. Fig. 14 presents the mean signal intensity of the channels (averaged across all 104 channels at a given flow rate) as a function of the mean flow rate through a single channel (total flow rate divided by 104). Signal intensity at zero flow rate

was measured at the probe-MSB distance of 150 μm along several rows and the average value was used. There is good consistency among the averaged signal intensities from different experiments under similar flow rates. Eq. 5 is fitted to the data and the fit is considered to be sufficiently good to be used. While A is the signal intensity at zero flow velocity to the power of two, B is obtained from the best fit.

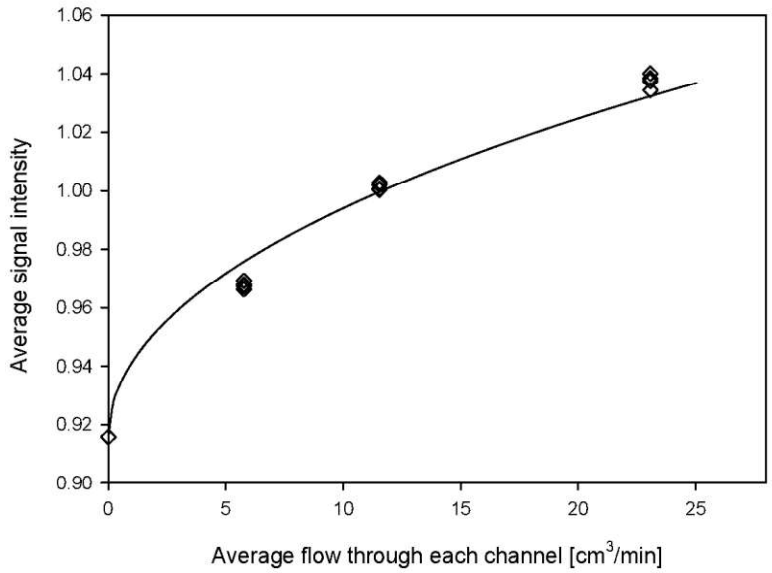

Figure 14: Mean signal intensity (voltage) derived from averaged signal across all channels at a given flow rate) as a function of average flow rate through a single channel. Solid line shows the best fit for Eq. 5.

Averaging the signal intensities across all channels is expected to create a larger inaccuracy when the flow through channels, and hence the signal intensity corresponding to it, varies largely among the channels at a given flow rate. This is the case for the measurements using wide catalyst size distribution (50-200 μm). Therefore, these data points are not used for calibration of the probe in Fig. 14.

All in all, while translating the signal intensities to absolute velocities may not be appropriate without more precise calibration of the probe, Eq. 5 is considered sufficiently precise for comparative study of the flow rate. Alternatively, a stepwise linear correlation between voltage and flow can be assumed, as applied by [Pfeifer and Schubert (2007)]. Such assumption may alter the intensities of the observed flow maldistribution, but would not affect

the main conclusions of this study.

4 Conclusion

Hot wire anemometry is used for experimental determination of the flow distribution in a micro-packed bed reactor for the first time, and the results obtained in air flow at ambient conditions are discussed in relation to the reactor performance for methanol synthesis under industrially relevant conditions (200-300 °C, 80 bar).

In the empty microstructured body (MSB), the flow distribution among the slits is uneven due to dimensional variations. The effect of fabrication tolerances is canceled out by catalyst particle filling, owing to a much higher pressure drop along the packed bed. However, nonuniform packing of the slits, promoted by the slit's design, widens the flow distribution in each slit. The flow rate is higher along the sidewalls of the slits, due to a less dense packing close to the walls. The flow distribution improves by using larger particles (up to 200 μm) with narrower size distribution, as well as by increasing the total flow rate and hence the pressure drop over the bed.

The effect of catalyst particle size on the methanol synthesis is investigated and established to be rather small under the conditions applied. The influence of particle size on the flow distribution might be much smaller than observed in the anemometry measurements due to a much lower flow velocity and pressure drop under the high pressure corresponding to the synthesis experiments. Moreover, such effects may even be balanced/dominated by effects of the pore diffusion on the apparent reaction rate.

According to the anemometry results, the flow distribution is expected to be wider at the methanol synthesis conditions (lower velocity) in the packed bed microreactor at low pressure drop. However, since the tiny outlet slits of the MSB (reactor body for anemometry) are not applied in the MSR (methanol synthesis reactor), the maldistribution could also be less with regard to the obtained reaction data. Syngas conversion is highly limited by thermodynamic equilibrium and methanol synthesis is highly exothermic over a catalyst which is prone to deactivation through thermal sintering. This can be seen as a huge driver for the application of microreactors to methanol syntheis or the like. Consequences of maldistribution could be significant on the reactor performance under the reaction in kinetic regime. However,

when the overall conversion is pushed towards equilibrium the differences in conversion levels in the individual channels get smaller, but an overall temperature increase does not help aleviating the difference. This should be solved by changing the reactor design. With regard to this issue, the results suggest a modification of the slits' margins to further promote uniform catalyst packing and even flow distribution.

Acknowledgment

The financial support from the Research Council of Norway (contract No. 208351/E30) is gratefully acknowledged.

References

[Bruun (1995)] H. H. Bruun , Hot-wire anemometry : principles and signal analysis , Oxford science publications, Oxford University Press , Oxford , 1995 .

[Dadgar et al. (2015)] F. Dadgar , R. Myrstad , P. Pfeifer , A. Holmen , H. J. Venvik , Direct dimethyl ether synthesis from synthesis gas: The influence of methanol dehydration on methanol synthesis reaction , Catalysis today 270 (2016) 76-84

[Pfeifer et al. (2004)] P. Pfeifer , A. Wenka , K. Schubert , M. A. Liauw , G. Emig , Characterization of flow distribution in microchannel reactors , AIChE Journal 50 (2004) 418–425 .

[Pfeifer and Schubert (2007)] P. Pfeifer , K. Schubert , Hot wire anemometry for experimental determination of flow distribution in multilayer microreactors , Chemical Engineering Journal 135 (2007) S173–S178 .

[Haughey and Beveridg (1969)] D. P. Haughey , G. S. G. Beveridg , Structural properties of packed beds - a review , Canadian Journal of Chemical Engineering 47 (1969) 130–140 .

[Ergun (1952)] S. Ergun , Fluid flow through packed columns , Chemical Engineering Progress 48 (1952) 89–94 .

[Pohar and Plazl (2009)] A. Pohar , I. Plazl , Process intensification through microreactor application , Chemical and Biochemical Engineering Quarterly 23 (2009) 537–544 .

[Mills et al. (2007)] P. L. Mills , D. J. Quiram , J. F. Ryley , Microreactor technology and process miniaturization for catalytic reactions - a perspective on recent developments and emerging technologies , Chemical Engineering Science 62 (2007) 6992–7010 .

[Borovinskaya and Reshetilovskii (2008)] E. S. Borovinskaya , V. P. Reshetilovskii , Microstructural reactors: Concept, development and application , Russian Journal of Applied Chemistry 81 (2008) 2211–2231 .

[Commenge etal. (2002)] J. M. Commenge , L. Falk , J. P. Corriou , M. Matlosz , Optimal design for flow uniformity in microchannel reactors , Aiche Journal 48 (2002) 345–358 .

[Matlosz and Commenge (2002)] M. Matlosz , J. M. Commenge , From process miniaturization to structured multiscale design: The innovative, high-performance chemical reactors of tomorrow , Chimia 56 (2002) 654–656 .

[Rebrov et al. (2007)] E. V. Rebrov , R. P. Ekatpure , M. H. J. M. de Croon , J. C. Schouten , Design of a thick-walled screen for flow equalization in microstructured reactors , Journal of Micromechanics and Microengineering 17 (2007) 633–641 .

[Mies et al. (2007)] M. J. M. Mies , E. V. Rebrov , L. Deutz , C. R. Kleijn , M. H. J. M. de Croon , J. C. Schouten , Experimental validation of the performance of a

microreactor for the high-throughput screening of catalytic coatings , Industrial & Engineering Chemistry Research 46 (2007) 3922–3931 .

[Lommerts et al. (2000)] B. J. Lommerts , G. H. Graaf , A. A. C. M. Beenackers , Mathematical modeling of internal mass transport limitations in methanol synthesis , Chemical Engineering Science 55 (2000) 5589–5598 .

[Graaf et al. (1990)] G. H. Graaf , H. Scholtens , E. J. Stamhuis , A. A. C. M. Beenackers , Intraparticle diffusion limitations in low-pressure methanol synthesis , Chemical Engineering Science 45 (1990) 773–783 .

[Hayer et al. (2013)] F. Hayer , H. Bakhtiary-Davijany , R. Myrstad , A. Holmen , P. Pfeifer , H. J. Venvik , Characteristics of integrated micro packed bed reactor-heat exchanger configurations in the direct synthesis of dimethyl ether , Chemical Engineering and Processing: Process Intensification 70 (2013) 77–85 .

[Bakhtiary-Davijany et al. (2012)] H. Bakhtiary-Davijany , F. Dadgar , F. Hayer , X. K. Phan , R. Myrstad , H. J. Venvik , P. Pfeifer , A. Holmen , Analysis of external and internal mass transfer at low reynolds numbers in a multiple-slit packed bed microstructured reactor for synthesis of methanol from syngas , Industrial & Engineering Chemistry Research 51 (2012) 13574–13579 .

[Bakhtiary-Davijany et al. (2011-1)] H. Bakhtiary-Davijany , F. Hayer , X. K. Phan , R. Myrstad , P. Pfeifer , H. J. Venvik , A. Holmen , Performance of a multi-slit packed bed microstructured reactor in the synthesis of methanol: Comparison with a laboratory fixed-bed reactor , Chemical Engineering Science 66 (2011 a) 6350–6357 .

[Bakhtiary-Davijany et al. (2011-2)] H. Bakhtiary-Davijany , F. Hayer , X. K. Phan , R. Myrstad , H. J. Venvik , P. Pfeifer , A. Holmen , Characteristics of an integrated micro packed bed reactor-heat exchanger for methanol synthesis from syngas , Chemical

Engineering Journal 167 (2011 b) 496–503 .

[Hayer et al. (2011-1)] F. Hayer , H. Bakhtiary-Davijany , R. Myrstad , A. Holmen , P. Pfeifer , H. J. Venvik , Synthesis of dimethyl ether from syngas in a microchannel reactor: Simulation and experimental study , Chemical Engineering Journal 167 (2011 a) 610–615 .

[Hayer et al. (2011-2)] F. Hayer , H. Bakhtiary-Davijany , R. Myrstad , A. Holmen , P. Pfeifer , H. J. Venvik , Modeling and simulation of an integrated micro packed bed reactor-heat exchanger configuration for direct dimethyl ether synthesis , Topics in Catalysis 54 (2011 b) 817–827 .

[Myrstad et al. (2009) Myrstad, Eri, Pfeifer, Rytter, and Holmen] R. Myrstad , S. Eri , P. Pfeifer , E. Rytter , A. Holmen , Fischer-tropsch synthesis in a microstructured reactor , Catalysis Today 147 (2009) S301–S304 .

[King (1914)] L. V. King , On the convection of heat from small cylinders in a stream of fluid: Determination of the convection constants of small platinum wires with applications to hot-wire anemometry , Philosophical Transactions of the Royal Society of London A: Mathematical, Physical and Engineering Sciences 214 (1914) 373–432 .